



Natural magnetite as an effective and long-lasting catalyst for CWPO of azole pesticides in a continuous up-flow fixed-bed reactor

Neus Lopez-Arago¹ · Macarena Munoz¹ · Zahara M. de Pedro¹ · Jose A. Casas¹

Received: 25 September 2023 / Accepted: 20 March 2024 / Published online: 3 April 2024
© The Author(s) 2024

Abstract

The global occurrence of micropollutants in water bodies has raised concerns about potential negative effects on aquatic ecosystems and human health. EU regulations to mitigate such widespread pollution have already been implemented and are expected to become increasingly stringent in the next few years. Catalytic wet peroxide oxidation (CWPO) has proved to be a promising alternative for micropollutant removal from water, but most studies were performed in batch mode, often involving complex, expensive, and hardly recoverable catalysts, that are prone to deactivation. This work aims to demonstrate the feasibility of a fixed-bed reactor (FBR) packed with natural magnetite powder for the removal of a representative mixture of azole pesticides, recently listed in the EU Watch Lists. The performance of the system was evaluated by analyzing the impact of H₂O₂ dose (3.6–13.4 mg L⁻¹), magnetite load (2–8 g), inlet flow rate (0.25–1 mL min⁻¹), and initial micropollutant concentration (100–1000 µg L⁻¹) over 300 h of continuous operation. Azole pesticide conversion values above 80% were achieved under selected operating conditions ($W_{\text{Fe}_3\text{O}_4} = 8 \text{ g}$, $[\text{H}_2\text{O}_2]_0 = 6.7 \text{ mg L}^{-1}$, flow rate = 0.5 mL min⁻¹, pH₀ = 5, $T = 25 \text{ }^\circ\text{C}$). Notably, the catalytic system showed a high stability upon 500 h in operation, with limited iron leaching (< 0.1 mg L⁻¹). As a proof of concept, the feasibility of the system was confirmed using a real wastewater treatment plant (WWTP) effluent spiked with the mixture of azole pesticides. These results represent a clear advance for the application of CWPO as a tertiary treatment in WWTPs and open the door for the scale-up of FBR packed with natural magnetite.

Keywords Azole pesticides · Fixed-bed reactor · Magnetite · Decision 2022/1307 · CWPO

Abbreviations

CWPO	Catalytic wet peroxide oxidation	Log k_{ow}	Octanol-water partition coefficient
FBR	Fixed-bed reactor	TOC (mg L ⁻¹)	Total organic carbon
WWTP	Wastewater treatment plant	IC (mg L ⁻¹)	Inorganic carbon
EU	European Union	Q (mL min ⁻¹)	Flow rate
AOPs	Advanced oxidation processes	W (g _{cat})	Catalyst load
TEB	Tebuconazole	τ (g _{cat} min mL ⁻¹)	Space-time
TET	Tetraconazole	Ca	Carberry number
PEN	Penconazole	$(-r_i)_{\text{obs}}$ (mg g _{cat} ⁻¹ min ⁻¹)	Observed reaction rate
XRD	X-ray diffraction	$k_{i,s}$	Liquid-solid mass transfer coefficient
SEM	Scanning electron microscope	k_{app} (mL g _{cat} ⁻¹ min ⁻¹)	Apparent kinetic constant
pH _{PZC}	Point of zero charge	a_v (m ² m ⁻³)	Volumetric external surface area
		$F_{i,0}$ (mg min ⁻¹)	Mass flow rate
		$C_{i,0}$ (mg L ⁻¹)	Pollutant concentration in the inlet stream
		C_i (mg L ⁻¹)	Pollutant concentration in the outlet stream

Responsible Editor: Angeles Blanco

✉ Neus Lopez-Arago
neus.lopez@uam.es

¹ Chemical Engineering Department, Universidad Autónoma de Madrid, Ctra. Colmenar Km 15, 28049 Madrid, Spain

Introduction

The worldwide occurrence of micropollutants in water resources represents a potential threat for aquatic ecosystems and human health (Figuère et al. 2022; Miyawaki et al. 2021). This vast array of anthropogenic compounds including pesticides, hormones, pharmaceuticals, personal care products, and industrial chemicals (Ahmed et al. 2017) is mainly introduced into the aquatic environment through wastewater treatment plants (WWTPs), which cannot warrant their complete elimination (Ben et al. 2018; García et al. 2021). With the aim to protect nature and human health from the most relevant micropollutants based on up-to-date scientific insights, the European Union (EU) has launched their control in EU water basins, urging its Member States to analyze the occurrence of the micropollutants included in the EU Watch Lists since 2015 (Decisions 2015/495, 2018/840, 2020/1161, and 2022/1307). These Watch Lists will be the basis for the upcoming review of the Urban Wastewater Treatment Directive, which will certainly limit the discharge of the most harmful substances. A particular case of hazardous micropollutants is the family of azole pesticides, included in the most recent EU Watch Lists (Decisions 2020/1161 and 2022/1307). These substances are increasingly applied as fungicides to control plant diseases, with a value share of 20–25% of the global fungicide volume market (Jørgensen & Heick 2021). Once in the aquatic environment, azole pesticides cause toxic effects on different living organisms like algae and fish (Chen & Ying 2015; Pesce et al. 2016; Poulsen et al. 2015; Storck et al. 2018).

The development of innovative but also highly effective, sustainable, inexpensive, and technically feasible water treatment systems that allow to create an absolute barrier to micropollutant emission at WWTPs represents a task of high priority nowadays. Advanced oxidation processes (AOPs), based on the in situ generation of strong and non-selective oxidizing radicals, appear as promising alternatives for such goal (Saravanan et al. 2021). Heterogeneous Fenton oxidation, also known as catalytic wet peroxide oxidation (CWPO), is particularly attractive as it combines the advantages of conventional homogeneous Fenton, *i.e.*, inexpensive chemicals, simple implementation, and mild conditions, with those of heterogeneous catalysis, *i.e.*, catalyst reusability and limited formation of iron sludge. In our previous contributions, we found that natural magnetite (Fe_3O_4), an inexpensive, sustainable, and highly available mineral, is an outstanding CWPO catalyst for the removal of a wide range of micropollutants included in the EU Watch Lists like macrolide antibiotics, hormones, diclofenac, neonicotinoid pesticides, and, very recently, azole pesticides (Lopez-Arago et al. 2023; Serrano et al. 2019, 2020). The latter were the lowest reactive towards CWPO, and thus, they are good

candidates to be used as general indicators of the overall efficiency of the catalytic system.

The effectiveness of CWPO for micropollutant removal has been extensively demonstrated in a discontinuous operation context (*i.e.*, slurry batch reactors) due to the easiness of operation and the fast operational parameters screening, but the laborious recovery and recirculation of the powdered catalyst particles clearly hinders its practical implementation considering the large volumes of wastewater treated at WWTPs. These requirements represent the most important challenge to the state-of-the-art on CWPO, where continuous operation has been remarkably less investigated, and pilot plant studies are practically inexistent. A comprehensive review devoted to the application of continuous reactors (fixed bed, fluidized bed, and continuous stirred-tank reactors) in CWPO was developed by Esteves et al. (2016), where fixed-bed reactors (FBR) were pointed as attractive configurations as they allow amplifying the solid/liquid ratio and thus, accelerating the oxidation rate while reducing the contact times. Furthermore, when compared to the other continuous systems, the residence time is well controlled with minimum back mixing, and loss, as well as mechanical crushing of the catalyst, are avoided to a high extent.

Table 1 collects the most recent works (last 5 years) focused on the application of CWPO in continuous FBRs. As can be seen, iron oxide catalysts are the most relevant solids applied in this process. In particular, those based on synthesized magnetite have received major attention, which can be attributed to the presence of both Fe(II) and Fe(III) species, which significantly fasten the oxidation rate (Munoz et al. 2015). In general, catalysts preparation involves the use of synthetic organic or inorganic supports and requires relatively complex multi-step procedures like incipient wetness impregnation followed by high-temperature calcination (di Luca et al. 2018; Ding et al. 2020), combination of thermal treatments and metal–organic chemical vapor deposition (Yang et al. 2018), clay intercalation by auto-hydrolysis followed by calcination (Pinchao et al. 2021) or chemical co-precipitation and hydrothermal treatment (Huacalco-Aguilar et al. 2021a, b; Huacalco-Aguilar et al. 2021a, b). There are also attempts using different kinds of wastes as carbon support precursors like PET bottles (Thirumoorthy et al. 2021) or olive stones (Esteves et al. 2022), but in both cases, complex multi-step procedures and carbonization at high temperatures were required. Catalyst preparation clearly increases the cost of CWPO application, but what is even more important, synthetic catalysts usually suffer from deactivation. In fact, catalyst deactivation is one of the main concerns dealing with the application of CWPO in continuous mode. Leaching of iron, fouling of the catalytic surface, poisoning, and pore blocking are the main reasons behind this undesirable phenomenon (di Luca et al. 2018). As can be appreciated in Table 1, most reported catalysts suffer

Table 1 Recent studies (2018–2023) focused on the application of CWPO in continuous FBRs

Catalyst	Target pollutant	Water matrix	Operating conditions	Main results (steady state)	Time on stream	Stability issues	Reference
Fe(III)-Al ₂ O ₃ (6 wt% Fe)	Phenol	Deionized water	$C_{\text{cont-H}_2\text{O}_2} = 1\text{--}6.1 \text{ g L}^{-1}$ $W_{\text{cat}} = 20 \text{ g}$ $T = 90 \text{ }^\circ\text{C}$ Flow rate = 1.2 mL min^{-1} $P = 1 \text{ atm}$ $\text{pH}_0 = 3$	$X_{\text{cont}} = 100\%$ $X_{\text{TOC}} = 90\%$	70 h	Iron leaching as main reason for deactivation. Attributed to chelating acidic intermediates Dissolved iron < 3 mg L^{-1} Cumulative iron loss = 20% of the initial load	di Luca et al. (2018)
Iron-loaded microfibrillar entrapped carbon-nanotube catalyst (Fe ₂ O ₃ -MF-CNT) (0.6 wt% Cu)	m-cresol	Deionized water	$C_{\text{cont-H}_2\text{O}_2} = 1\text{--}6 \text{ g L}^{-1}$ $T = 60 \text{ }^\circ\text{C}$ Flow rate = 6 mL min^{-1} $P = 1 \text{ atm}$ $\text{pH}_0 = 5$	$X_{\text{cont}} > 95\%$ $X_{\text{COD}} = 30\%$	24 h	Slight deactivation Low-iron leaching (quantitative results are not provided)	Yang et al. (2018)
Pelletized Cu catalysts (Cu/ γ -Al ₂ O ₃) (1.5 wt% Cu)	Methyl orange	Deionized water	$C_{\text{cont-H}_2\text{O}_2} = 9.81\text{--}986 \text{ mg L}^{-1}$ $W_{\text{cat}} = 9.9 \text{ g}$ $T = 50 \text{ }^\circ\text{C}$ Flow rate = 2 mL min^{-1} $P = 1 \text{ atm}$ $\text{pH}_0 = 8.2$	$X_{\text{cont}} > 95\%$ $X_{\text{COD}} > 95\%$	200 h	Relatively high stability Dissolved copper = 0.4 mg L^{-1} Cumulative copper loss = 2.7% of the initial load	Ding et al. (2020)
Monolayer graphene film	Phenol	Deionized water	$C_{\text{cont-H}_2\text{O}_2} = 1\text{--}5.1 \text{ g L}^{-1}$ $W_{\text{cat}} = 4.8 \text{ g}$ $T = 80 \text{ }^\circ\text{C}$ Flow rate = 2 mL min^{-1} $P = 1 \text{ atm}$ $\text{pH}_0 = 6$	$X_{\text{cont}} = 100\%$ $X_{\text{TOC}} = 80\text{--}90\%$	72 h	High stability with steady conversion along the long-term experiment	Liu et al. (2020)
Al/Fe-pillared clay (0.5 wt% Fe)	Natural organic matter	Deionized water	$C_{\text{TOC-H}_2\text{O}_2} = 10\text{--}472 \text{ mg L}^{-1}$ $W_{\text{cat}} = 27 \text{ g}$ $T = 20 \text{ }^\circ\text{C}$ Flow rate = 8 mL min^{-1} $P = 1 \text{ atm}$ $\text{pH}_0 = 7.2$	$X_{\text{TOC}} = 24\%$	30 h (3 h each run)	Dissolved iron < 0.15 mg L^{-1} Estimated cumulative iron loss = 1.6% of the initial load	Pinchao et al. (2021)

Table 1 (continued)

Catalyst	Target pollutant	Water matrix	Operating conditions	Main results (steady state)	Time on stream	Stability issues	Reference
Fe ₃ O ₄ /multi-walled carbon nanotubes (25.4 wt% Fe)	Diclofenac and ibuprofen	Deionized water Surface water WWTP effluent Hospital wastewater effluent	$C_{\text{diclofenac-ibuprofen-H2O2}} = 11.9\text{--}10.2\text{--}104.5 \text{ mg L}^{-1}$ $W_{\text{cat}} = 0.4 \text{ g}$ $T = 60 \text{ }^\circ\text{C}$ Flow rate = 1 mL min ⁻¹ $P = 1 \text{ atm}$ $pH_0 = 5$	$X_{\text{Diclofenac}} = 95\%$ $X_{\text{Ibuprofen}} = 90\%$ $X_{\text{TOC}} = 71\%$	20 h	Slight deactivation along 3 consecutive uses of 3 h time on stream Information about iron leaching not provided	Huacalco-Aguilar et al. (2021b)
Fe ₃ O ₄ /multi-walled carbon nanotubes (25.4 wt% Fe)	Naproxen	Deionized water Surface water WWTP effluent Hospital wastewater effluent	$C_{\text{cont-H2O2}} = 10\text{--}95 \text{ mg L}^{-1}$ $W_{\text{cat}} = 0.4 \text{ g}$ $T = 50 \text{ }^\circ\text{C}$ Flow rate = 1.7 mL min ⁻¹ $P = 1 \text{ atm}$ $pH_0 = 6.3$	$X_{\text{cont}} = 78\%$ $X_{\text{TOC}} = 83\%$	24 h	Iron leaching as main reason for slight deactivation Dissolved iron = 0.28 mg L ⁻¹ Cumulative iron loss = 15% of the initial load	Huacalco-Aguilar et al. (2021a)
Al-doped magnetite spinel nanoparticles encapsulated in mesoporous carbon (21%γ-Fe ₂ O ₃ /28%FeAl ₂ O ₄ @MC)	Phenol	Deionized water	$C_{\text{cont-H2O2}} = 0.2\text{--}1.2 \text{ g L}^{-1}$ $W_{\text{cat}} = 0.1 \text{ g}$ $T = 40 \text{ }^\circ\text{C}$ Flow rate = 0.1 mL min ⁻¹ $P = 1 \text{ atm}$ $pH_0 = 3$	$X_{\text{TOC}} = 80\%$	500 h	Relatively high stability despite metal leaching Dissolved iron = 1 mg L ⁻¹ (up to 2 mg L ⁻¹ along the first 200 h on stream) Dissolved aluminum = 2 mg L ⁻¹	Thirumoorthy et al. (2021)
Iron oxide supported on activated carbon prepared from olive stones (5 wt% Fe)	Phenolic compounds Real olive mill wastewater	Deionized water Real olive mill wastewater	$C_{\text{cont-H2O2}} = 0.34\text{--}1.2 \text{ g L}^{-1}$ (phenolic compounds) $C_{\text{cont-H2O2}} = 1.25\text{--}2.75 \text{ g L}^{-1}$ (olive mill wastewater) $W_{\text{cat}} = 1 \text{ g}$ $T = 60 \text{ }^\circ\text{C}$ Flow rate = 0.75 mL min ⁻¹ $P = 1 \text{ atm}$ $pH_0 = 3.5$ (phenolic compounds) $pH_0 = 4.5$ (olive mill wastewater)	Phenolic compounds: $X_{\text{cont}} = 87\%$ $X_{\text{TOC}} = 28\%$ Real olive mill wastewater: $X_{\text{cont}} = 57\text{--}71\%$ $X_{\text{COD}} = 26\text{--}34\%$	48 h	Iron leaching as main reason for deactivation Cumulative iron loss = 9% of the initial loss Full catalytic activity for 36 h	Esteves et al. (2022)

Table 1 (continued)

Catalyst	Target pollutant	Water matrix	Operating conditions	Main results (steady state)	Time on stream	Stability issues	Reference
Natural magnetite	Azole pesticides mixture (tebuconazole, tetraconazole and penconazole)	Deionized water WWTP effluent	$C_{\text{cont}}(\text{each})\text{-H}_2\text{O}_2 = 0.5\text{--}6.7 \text{ mg L}^{-1}$ $W_{\text{cat}} = 8 \text{ g}$ $T = 25 \text{ }^\circ\text{C}$ Flow rate = 0.5 mL min^{-1} $P = 1 \text{ atm}$ $\text{pH}_0 = 5$	$X_{\text{tebuconazole}} = 93\%$ $X_{\text{tetraconazole}} = 78\%$ $X_{\text{penconazole}} = 85\%$	500 h	High stability Dissolved iron < 0.2 mg L^{-1} Cumulative iron loss < 0.05% of the initial load	This work

deactivation to some extent, being iron leaching as the most important cause for the activity loss. A metal-free catalyst based on a monolayer graphene film showed a reasonably good stability, but it exhibited a relatively low activity as denoted by the high operating temperature applied ($80 \text{ }^\circ\text{C}$) (Liu et al. 2020). On the other hand, it must be noted that most CWPO applications were focused on the treatment of aromatic compounds as well as dyes and industrial wastewaters at relatively high pollutant concentrations ($\text{mg L}^{-1}\text{--g L}^{-1}$). Studies focused on the abatement of micropollutants are scarce and carried out at pollutant concentrations clearly higher than the representative concentration at WWTP effluents (Huacalco-Aguilar et al. 2021a, b; Huacalco-Aguilar et al. 2021a, b). Furthermore, most works were performed at relatively high operating temperature ($50\text{--}90 \text{ }^\circ\text{C}$), and long-term studies are limited, with most publications testing time on stream of 1–3 days. All in all, there exists a noticeable knowledge gap regarding the development and application of robust and stable catalysts in CWPO in long-term operation. These studies are urgently required to demonstrate the feasibility of this system for potential application in WWTPs as tertiary treatment for micropollutant removal.

The application of pristine magnetite mineral as catalyst could overcome the main shortcomings of synthetic catalysts in a unique manner as iron is part of the robust mineral structure, and thus, it is highly stable, with limited iron leaching (Munoz et al. 2018). Furthermore, its low surface area and practically negligible adsorption capacity for organic compounds would minimize possible poisoning, fouling, and pore blocking, as demonstrated in previous batch operation studies (Lopez-Arago et al. 2023; Serrano et al. 2019, 2020). Despite these advantages, to the best of our knowledge, pristine magnetite mineral has not been tested as a catalyst in continuous FBR so far.

The aim of this work is to demonstrate the feasibility of a FBR packed with natural magnetite powder for the CWPO of a representative mixture of azole pesticides (tebuconazole (TEB), tetraconazole (TET), and penconazole (PEN)) listed in the most recent EU Watch Lists (Decision 2020/1161 and Decision 2022/1307). This work clearly represents a significant advancement in the context of the literature, as it proves the viability of CWPO in long-term operation (500 h). The catalytic performance of the system was evaluated analyzing the impact of the main operating parameters, i.e., catalyst load, feed flow rate, hydrogen peroxide dose, and initial micropollutants concentration along 300 h on stream. To warrant the practical applicability of the catalytic system, all experiments were performed under ambient conditions. In the same line, a slightly acidic pH value ($\text{pH}_0 = 5$) was established to maximize the H_2O_2 consumption efficiency, as demonstrated in our previous work in batch reactor operation (Munoz et al. 2018). Under optimized conditions, an additional long-term experiment for 200 h was performed

to further demonstrate the high stability of the FBR packed with natural magnetite powder. As a proof of concept, a real WWTP sample fortified with the micropollutants mixture was finally employed as the inlet stream. These results represent an important step forward in the field of CWPO and open the door for its scale-up.

Materials and methods

Materials and chemicals

Azole pesticides (analytical grade quality), hydrogen peroxide solution (33% wt.), nitric acid (65%), and hydroxylamine ($\geq 99\%$) were obtained by Sigma-Aldrich. Acetonitrile (99.9%) and 1,10-phenanthroline ($\geq 99\%$) were provided from Scharlau and Fluka, respectively. All reagents were used without further purification. The magnetite mineral powder employed as catalyst (ref: 500121500) was provided by Marphil S.L. (Spain). Natural magnetite granules (ref: 0029882796573), used to pack the magnetite powder in the FBR, were supplied by Inoxia (UK). Unless otherwise indicated, all trials were conducted using deionized water. The main properties of the azole pesticides tested in this work are summarized in Table 2.

Catalyst characterization

The complete characterization of the powdered natural magnetite (Fe_3O_4) catalyst employed in this work can be found in our previous contribution (Munoz et al. 2018). Crystalline magnetite was the only phase present in the solid according to XRD analysis, being the content of iron similar to the theoretical one for pure magnetite (73 wt%). Consistent with these features, the solid showed strong magnetic properties

($M_S = 77.9 \text{ emu g}^{-1}$). The average size of the particles, which showed a rough spheric shape, was $0.2 \mu\text{m}$, being the specific surface area value of $7 \text{ m}^2 \text{ g}^{-1}$. The point of zero charge (pH_{PZC}) was 7.8.

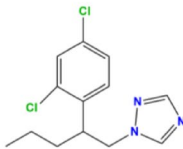
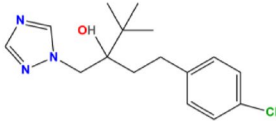
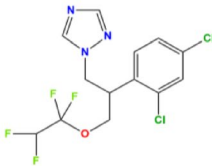
Furthermore, SEM images for both natural and used magnetite after 500 h of continuous operation were acquired using a JSM 6335F microscope (JEOL Ltd., Tokyo, Japan).

Experimental procedure

The experimental setup used in this work is shown in Fig. 1. The FBR consists of a jacketed glass column (18 mm i.d., 115 mm length) where the catalyst bed (Fe_3O_4 , $0.2 \mu\text{m}$) was packed between two layers of magnetite granules. The bottom layer (Fe_3O_4 , 1.5 g, $250\text{--}500 \mu\text{m}$) was employed to improve aqueous solution dispersion in the catalytic bed. The top layer (Fe_3O_4 , 6 g, $500\text{--}1000 \mu\text{m}$) was added to prevent the possible loss of the fine catalyst powder taking advantage of the magnetic properties of both solids. These three layers were placed between two layers of glassy beads ($2\text{--}3 \text{ mm}$) and a fine layer of glass wool. The reactor was continuously fed in up-flow mode using a peristaltic pump to prevent gas pocket formation and ensure that the catalyst powder is totally wetted.

CWPO trials were performed under ambient conditions (1 atm, $25 \text{ }^\circ\text{C}$) at a slightly acidic pH value ($\text{pH}_0 = 5.0$), which was adjusted with HNO_3 (1 M). Operating temperature was kept constant by the upstream circulation of tempered water ($25 \text{ }^\circ\text{C}$) throughout the column jacket. The main parameters of the process were systematically investigated along 300 h on stream. The impact of each operating condition was assessed under steady-state conditions, and the experiments have an approximate duration of 24 h. Samples were taken from the reactor effluent every

Table 2 Main properties of the azole pesticides

	Penconazole (PEN)	Tebuconazole (TEB)	Tetraconazole (TET)
CAS number	66246-88-6	107534-96-3	112281-77-3
Molecular formula	$\text{C}_{13}\text{H}_{15}\text{Cl}_2\text{N}_3$	$\text{C}_{16}\text{H}_{22}\text{ClN}_3\text{O}$	$\text{C}_{13}\text{H}_{11}\text{Cl}_2\text{F}_4\text{N}_3\text{O}$
Structural formula			
Molar weight (g mol^{-1})	284.2	307.8	372.1
pK_a^a	5.2	5.0	0.7
$\text{Log } k_{ow}^a$	3.72	2.70	3.56

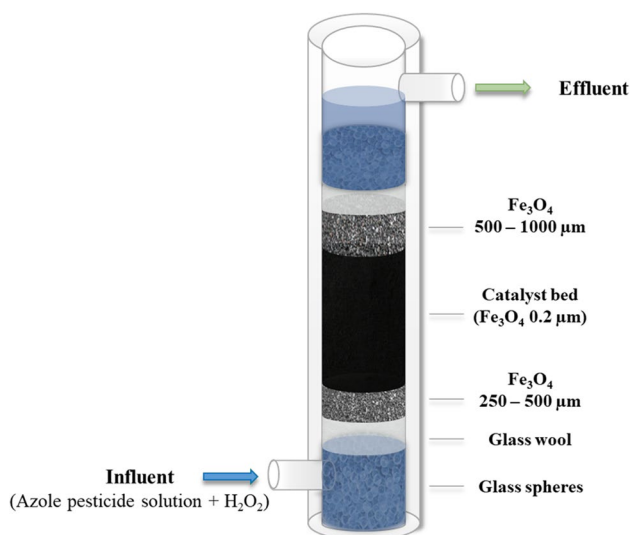


Fig. 1 Scheme of the FBR packed with powdered magnetite catalyst used in the continuous CWPO experiments

1 h. Accordingly, the effect of catalyst weight in the bed (2–8 g), the reactor inlet flow rate ($0.25\text{--}1\text{ mL min}^{-1}$), the hydrogen peroxide dose ($3.4\text{--}13.4\text{ mg L}^{-1}$), and the initial pesticide concentration ($100\text{--}1000\text{ }\mu\text{g L}^{-1}$) were studied. As depicted in Fig. 1, both the mixture of azole pesticides and H_2O_2 at the desired concentrations were transferred into the reactor in the up-flow inlet stream. A long-term continuous experiment (200 h) was accomplished after evaluating the operating conditions. Finally, the impact of the water matrix composition was also studied using a real WWTP effluent. All experiments were performed in triplicate, and the standard deviation was below 12%.

Preliminary experiments allowed to discard the possible role of azole pesticides adsorption on the catalytic bed, as the decrease on their concentration was negligible in the absence of H_2O_2 . In the same line, it was also confirmed that H_2O_2 alone cannot efficiently oxidize the micropollutants under the operating conditions tested in this work (pesticide conversion $< 5\%$). Finally, it was demonstrated that the magnetite granules used to pack the reactor were practically inactive for the CWPO reaction given their significantly lower exposed surface area compared to the fine catalyst powder.

Analytical methods

Liquid samples were periodically taken from the reactor effluent along the continuous CWPO experiments. Azole pesticide concentration was determined by HPLC–UV (Shimadzu, Prominence-I model, LC-2030C LT) using an Agilent Eclipse Plus C18 column (15 cm length, 4.6 mm diameter) as stationary phase. A mixture of acetonitrile and ultrapure

water at 0.8 mL min^{-1} was used as the mobile phase (60/40%, v/v). The detection wavelength was set at 222 nm for all the pesticides. Dissolved iron concentration was quantified by colorimetry with a UV 2100 Shimadzu UV–VIS spectrophotometer using the *o*-phenantroline method (Hoffman 1945). Total organic carbon (TOC) was determined with a TOC analyzer (Shimadzu TOC V_{SCH}, Kyoto, Japan).

Results and discussion

Kinetic study

The possible existence of mass transfer limitations in the FBR packed with magnetite was evaluated prior to conducting the kinetic study. This preliminary analysis is crucial as mass transfer limitations lead to a performance decrease, increasing the operating costs (Alalm et al. 2021). For such study, the azole pesticide tebuconazole (TEB) was selected as a target pollutant since it is one of the most widely used triazole fungicides (Stamatis et al. 2015), being frequently detected in WWTP effluents in the order of ng L^{-1} (Stamatis et al. 2010). Moreover, as it will be shown in the following sections, TEB exhibited the highest reactivity among the three micropollutants tested in this work, although all of them showed removal yields above 80% in the optimum conditions. To check external mass transfer limitations in the reaction system, both the flow rate (Q) and catalyst load (W) were systematically varied, leading to different space–time values ($\tau = \frac{W}{Q}$) between 4 and $32\text{ g}_{\text{cat}}\text{ min mL}^{-1}$. The results obtained are collected in Fig. 2. The modification of the flow rate, keeping constant the catalyst load, is denoted by the solid symbols, while the variation of the catalyst load, keeping constant the flow rate, is denoted by the square ones. As can be seen, external mass transfer limitations can be discarded under the operating conditions tested in this work as the conversion of the pollutant was maintained practically unchanged for the same space–time when the catalyst load or the flow rate was varied.

To further confirm the absence of external mass transfer limitations in the FBR system, the Carberry number (Ca) was calculated for TEB, the pesticide which showed the highest reactivity. For such goal, Sherwood, Reynolds, and Schmidt numbers were used for the estimation of the liquid–solid mass transfer coefficient ($k_{\text{TEB},s}$) of the system (see Supplementary Material for details). The Carberry number represents the relationship between the observed reaction rate and the maximum external mass transfer rate (Eq. 1).

$$Ca = \frac{(-r_{\text{TEB}})_{\text{obs}}}{k_{\text{TEB},s} a_v C_{\text{TEB},s}} \quad (1)$$

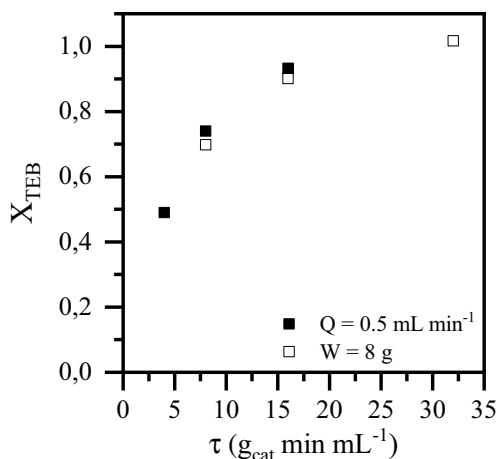


Fig. 2 Effect of τ variations (4–32 $g_{cat} \text{ min mL}^{-1}$) on TEB oxidation ($[TEB]_0 = 500 \mu\text{g L}^{-1}$; $W = 2\text{--}8 \text{ g}$; $Q = 0.25\text{--}1 \text{ mL min}^{-1}$; $[\text{H}_2\text{O}_2]_0 = 2.7 \text{ mg L}^{-1}$; $\text{pH}_0 = 5$; $T = 25 \text{ }^\circ\text{C}$)

where $(-r_{TEB})_{obs}$ is the observed reaction rate for TEB ($\text{mg L}^{-1} \text{ min}^{-1}$), $k_{TEB,s}$ is the corresponding liquid–solid mass transfer coefficient (m s^{-1}) for the micropollutant, a_v is the volumetric external surface area of the catalyst particles ($\text{m}^2 \text{ m}^{-3}$), and $C_{TEB,s}$ is the concentration (mg L^{-1}) of the micropollutant in the liquid phase. $(-r_{TEB})_{obs}$ was obtained experimentally, while $k_{TEB,s}$ was estimated using the Sherwood number (see Table S1 of the Supplementary Material). The obtained values for the Carberry number were far below 0.05 under steady-state conditions which confirmed the absence of mass transfer limitations at the operating conditions testing in this work (Vega et al. 2022).

The determination of the reaction kinetics was experimentally accomplished by varying the concentration of the pesticides in the inlet stream. As a representative example, it must be noted that the conversion values obtained by the FBR for TEB (X_{TEB}) at different starting micropollutant concentrations (from 100 to 1000 $\mu\text{g L}^{-1}$) were in the range of 93–97% (see Fig. S1 of the Supplementary Material).

Therefore, varying the initial concentration of the pesticide in the inlet stream did not cause any significant change in the conversion of the pollutant under steady-state conditions. Accordingly, the process can be described by a pseudo-first-kinetic-order model. Considering this aspect, the mass balance for a continuous fixed-bed reactor was applied to determine the apparent kinetic constant of the reaction (k_{app}) following Eq. 2.

$$\frac{W}{F_{i,o}} = \int_0^{X_i} \frac{dX_i}{(-r_i)_{obs}} \quad (2)$$

where W is the catalyst weight (g), $F_{i,0}$ is the mass flow rate of the pesticide fed to the reactor (mg min^{-1}), X_i is the pesticide conversion value, and $(-r_i)_{obs}$ is the reaction rate

of each pesticide ($\text{mg } g_{cat}^{-1} \text{ min}^{-1}$). Since a pseudo-first-kinetic-order model was proposed to describe the reaction, Eq. 2 can be rewritten as Eq. 3:

$$\frac{W}{QC_{i,o}} = \int_0^{X_i} \frac{dX_i}{k_{app}C_{i,t}} = \int_0^{X_i} \frac{dX_i}{k_{app}C_{i,0}(1-X_i)} \quad (3)$$

where Q is the flow rate (mL min^{-1}), $C_{i,0}$ and $C_{i,t}$ are the pollutant concentration in the inlet and outlet streams, respectively (mg mL^{-1}).

By the integration of Eq. 3, the value of the k_{app} ($\text{mL } g_{cat}^{-1} \text{ min}^{-1}$) can be obtained by plotting the experimental data according to Eq. 4:

$$\ln\left(\frac{1}{1-X_i}\right) = k_{app} \frac{W}{Q} \quad (4)$$

The k_{app} calculated values for PEN, TET, and TEB removal were 0.12 ± 0.03 , 0.09 ± 0.04 , and $0.17 \pm 0.03 \text{ mL } g_{cat}^{-1} \text{ min}^{-1}$, respectively, along the different space-times tested in this work (4–32 $g_{cat} \text{ min mL}^{-1}$). The apparent pseudo-first-order rate constants for the three azole pesticides under all the operation conditions tested in this work are collected in Fig. S2, S3, and S4 of the Supplementary Material.

Impact of operating conditions on FBR performance

The impact of the space–time on the stability of the FBR system for pesticide removal was evaluated in the range of 4–32 $g_{cat} \text{ min mL}^{-1}$, varying both the flow rate and the catalyst load. The results obtained are depicted in Fig. 3. The shading area in the figure denotes the time required to achieve the steady state. In the first place, it must be noted that the azole pesticide reactivity decreased following the order: TEB > PEN > TET, which is consistent with our previous contribution where the removal of azole pesticides by CWPO in batch operation was investigated (Lopez-Arago et al. 2023). This phenomenon may be attributed to the competitive effects among different pesticides, which can be influenced by their chemical structure and properties (Table 2). TEB only contains a chlorine substituent at the *-para* position, while both TET and PEN contain two chlorine radicals attached to the aromatic ring in the *-orto* and *-para* position. The presence of halogen substituents stabilizes the delocalized electrons of the aromatic ring and thus, TET and PEN showed a lower reactivity than TEB. On the other hand, the main reason for the slower degradation rate of TET may be explained by the fact that it has less alkyl groups in its structure (Rokbani et al. 2019).

As observed in Fig. 3, the system showed a high stability since the micropollutant conversion remained practically

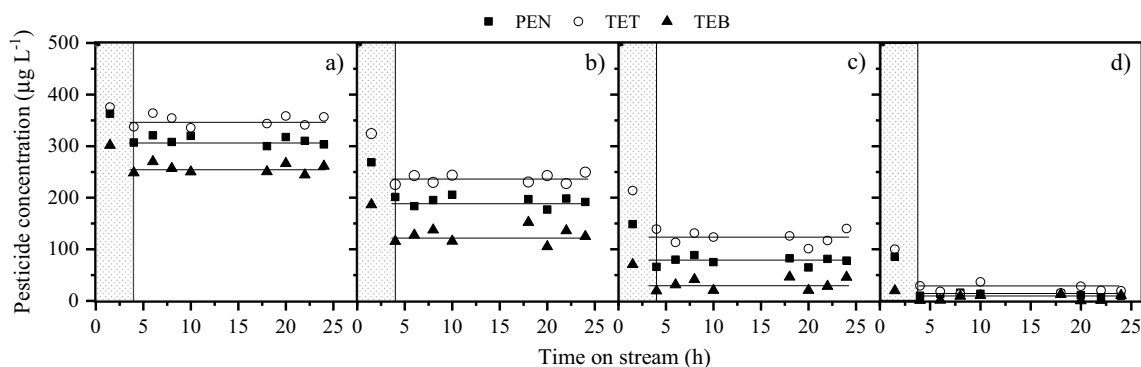


Fig. 3 Impact of space–time (a: $4 \text{ g}_{\text{cat}} \text{ min mL}^{-1}$; b: $8 \text{ g}_{\text{cat}} \text{ min mL}^{-1}$; c: $16 \text{ g}_{\text{cat}} \text{ min mL}^{-1}$; d: $32 \text{ g}_{\text{cat}} \text{ min mL}^{-1}$) on the oxidation of the three azole pesticides ($[\text{TET}]_0 = [\text{TEB}]_0 = [\text{PEN}]_0 = 500 \text{ } \mu\text{g L}^{-1}$; $[\text{H}_2\text{O}_2]_0 = 6.7 \text{ mg L}^{-1}$; $\text{pH}_0 = 5$; $T = 25 \text{ } ^\circ\text{C}$)

unchanged along 25 h-experiments. Besides, iron leaching was below 0.1 mg L^{-1} in the FBR effluent in all cases. The removal of the target pollutants clearly increased with increasing the space–time. For instance, the conversion of TET, the least reactive pesticide towards CWPO, increased from ~ 30 to $\sim 95\%$ by varying the space–time from 4 to $32 \text{ g}_{\text{cat}} \text{ min mL}^{-1}$. Under these conditions, *i.e.*, a flow rate of 0.25 mL min^{-1} and a catalyst amount of 8 g, a residence time of around 30 min is assumed, considering that the reaction volume (useful volume) was $\sim 8 \text{ mL}$. This residence time is quite attractive taking into account that 45 min is the average contact time in conventional adsorption tertiary treatment (Mailler et al. 2016).

It is well-known that H_2O_2 represents the main operating cost in Fenton-based technologies and thus, the optimization of its consumption is a critical issue that must be considered (Berberidou et al. 2022; Cai et al. 2020). Although the impact of this operating cost is clearly more evident in the treatment of highly polluted industrial wastewaters (Munoz et al. 2014; Pliego et al. 2012) than in the degradation of micropollutants, any decrease in its intake clearly favors the economy of the process.

Fig. 4 shows the results obtained in the continuous removal of azole pesticides by CWPO at different H_2O_2 doses. In particular, concentrations of 3.4, 6.7, 10.0, and 13.4 mg L^{-1} were tested, which approximately correspond to 50%, 100%, 150%, and 200% of the theoretical stoichiometric dose of H_2O_2 required to achieve the mineralization of the micropollutants. As observed, the conversion of the azole pesticides was slightly decreased when the stoichiometric dose of H_2O_2 was decreased by half. For instance, in the case of PEN, the conversion decreased from 85 to 71%. This result can be explained by the decrease in oxidizing species concentration under these conditions. Following the same trend, when the H_2O_2 dose was increased up to 150% of the theoretical stoichiometric amount, the conversion of the micropollutants was also increased. In this case, TEB conversion reached up to 97%. Nevertheless, a further increase of the H_2O_2 dose (up to 200% of the theoretical stoichiometric amount) led to a decrease of the azole pesticides conversion rate (e.g., TEB conversion was reduced to 88%). The concentration of H_2O_2 was then in clear excess so the oxidant itself could compete with the micropollutants

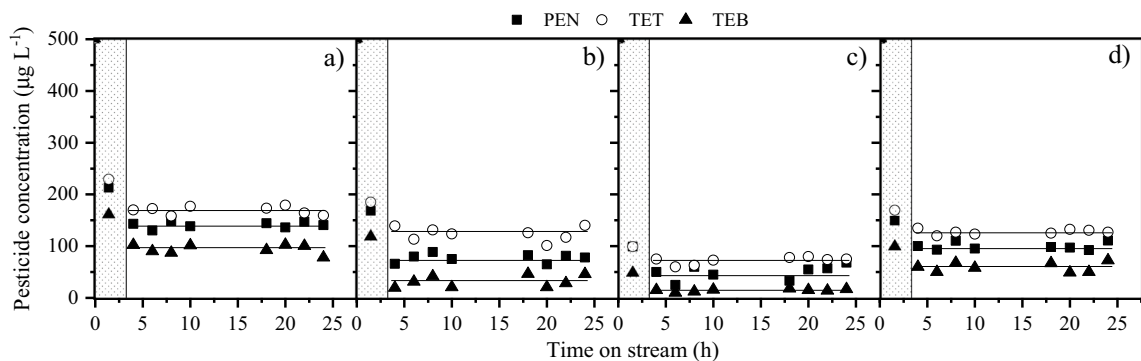
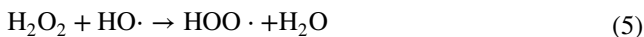


Fig. 4 Impact of the H_2O_2 initial concentration (a: 3.6 mg L^{-1} ; b: 6.7 mg L^{-1} ; c: 10.0 mg L^{-1} ; d: 13.4 mg L^{-1}) on the oxidation of the three azole pesticides ($[\text{TET}]_0 = [\text{TEB}]_0 = [\text{PEN}]_0 = 500 \text{ } \mu\text{g L}^{-1}$; $\tau = 16 \text{ g}_{\text{cat}} \text{ min mL}^{-1}$; $\text{pH}_0 = 5$; $T = 25 \text{ } ^\circ\text{C}$)

for the available active sites at the catalytic surface, leading to an inefficient consumption of H_2O_2 and slower degradation of the pesticides (Farzaneh Kondori et al. 2018; Huacalco-Aguilar et al. 2021a, b). Furthermore, H_2O_2 could also act as an autoscavenger for oxidizing radicals (mainly $\text{HO}\cdot$ and $\text{HOO}\cdot$), leading to termination reactions, as the following ones (Eqs. 5–6) (Farzaneh Kondori et al. 2018; Pera-Titus et al. 2004):



The apparent pseudo-first-order rate constant values also showed the same trend, obtaining the highest value at 150% of the theoretical stoichiometric dose of H_2O_2 . For instance, the pseudo-first-order constant value obtained for the most reactive azole pesticide (TEB) was $0.22 \text{ mL } g_{\text{cat}}^{-1} \text{ min}^{-1}$. Nevertheless, this value was quite similar to the one achieved with the theoretical stoichiometric dose of H_2O_2 ($0.17 \text{ mL } g_{\text{cat}}^{-1} \text{ min}^{-1}$) and thus, this dose was selected for further studies. Finally, it must be highlighted that the modification of the H_2O_2 dose did not lead to any significant change on the stability of the catalytic bed, being the dissolved iron concentration below 0.1 mg L^{-1} under the different conditions tested.

FBR long-term stability

To assess the stability of the system, a long-term continuous experiment was carried out for 200 h on stream under selected operating conditions (τ of $16 \text{ g}_{\text{cat}} \text{ min mL}^{-1}$, initial azole pesticides concentration of $500 \text{ } \mu\text{g L}^{-1}$ and H_2O_2 dose of 6.7 mg L^{-1}). As can be seen in Fig. 5, the FBR packed with magnetite showed an outstanding stability over 200 h on stream with no significant changes in the conversion values achieved for the azolic pesticides along the experiment. In fact, the main properties of the catalyst remained practically unchanged after being used. The absence of significant carbonaceous deposits on the surface of the used catalyst was confirmed, as the carbon content was determined to be less than 0.1 wt%. Additionally, it was observed that the specific surface area value and magnetic properties were practically the same as the measured for the fresh material. As a representative example, Fig. 6 shows a comparison between fresh (Fig. 6a) and used magnetite (Fig. 6b) SEM images after the long-term experiment. As can be seen, magnetite did not suffer any significant morphological change after 200 h of continuous treatment. Notably, the concentration of dissolved iron on the outlet stream was below 0.1 mg L^{-1} . After the whole experiment, less than 0.05 wt% of the iron contained in the catalyst was leached.

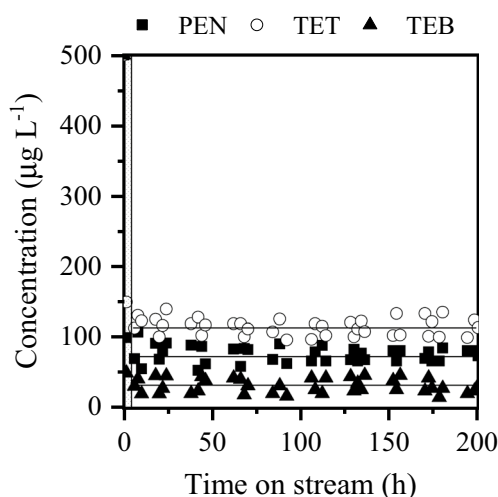


Fig. 5 Long-term performance of the catalytic fixed-bed reactor upon CWPO of the three azole pesticides ($[\text{TET}]_0 = [\text{TEB}]_0 = [\text{PEN}]_0 = 500 \text{ } \mu\text{g L}^{-1}$; $\tau = 16 \text{ g}_{\text{cat}} \text{ min mL}^{-1}$; $[\text{H}_2\text{O}_2]_0 = 6.7 \text{ mg L}^{-1}$; $\text{pH}_0 = 5$; $T = 25 \text{ } ^\circ\text{C}$)

Proof of concept

The influence of the water matrix composition on the overall efficiency of the CWPO process is an important issue to be considered as the presence of co-existing substances could compete with the pollutants for the active sites of the catalyst, lead to the fouling of the catalyst surface, or act as oxidizing radical scavengers (Garcia-Costa et al. 2021; Miklos et al. 2018). To evaluate such impact, the treatment of a real WWTP effluent sample, spiked with the mixture of azole pesticides at $500 \text{ } \mu\text{g L}^{-1}$, was evaluated. The main characteristics of the raw aqueous matrix are summarized in Table 3. The sample showed a relevant concentration of both organic and inorganic carbon sources. Furthermore, it also presented a non-negligible concentration of dissolved salts, being some of them common hydroxyl radical scavengers like chloride and sulfate (Lipczynska-Kochany et al. 1995; Lu et al. 2005; Siedlecka et al. 2007).

Given the relatively high organic matter load present in the real water matrix, the H_2O_2 concentration used in this experiment was 10 mg L^{-1} , while the space-time was kept at $16 \text{ g}_{\text{cat}} \text{ min mL}^{-1}$. The results obtained are shown in Fig. 7 where the k_{app} of each experiment was obtained. For the sake of comparison, the results achieved using deionized water are provided as well. Clearly, the process was less efficient in the WWTP effluent, leading to a decrease of the pollutant conversion at the same space-time from 85%, 78%, and 93% to 62%, 48%, and 75% for PEN, TET, and TEB, respectively. The decrease

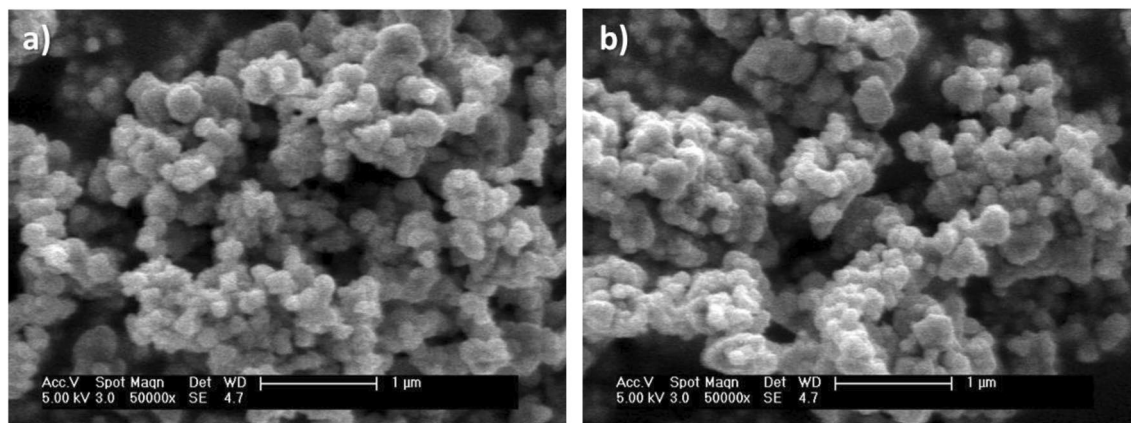


Fig. 6 SEM images of fresh (a) and used (b) magnetite

Table 3 Main characteristics of real water matrix tested

Parameter	Secondary WWTP effluent
pH	7.5
TOC (mg L^{-1})	6.3
IC (mg L^{-1})	12.1
Conductivity ($\mu\text{S cm}^{-1}$)	1182
Cl^{-} (mg L^{-1})	21.4
NO_3^{-} (mg L^{-1})	15.8
SO_4^{2-} (mg L^{-1})	197
PO_4^{3-} (mg L^{-1})	2.9

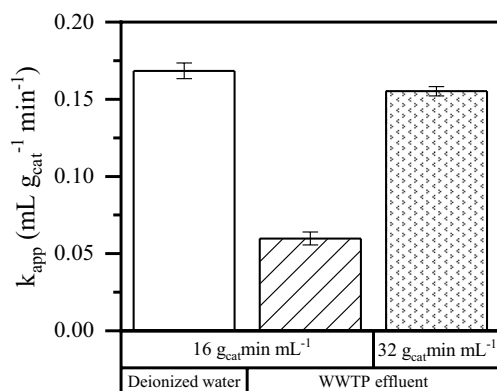


Fig. 7 Apparent pseudo-first-order kinetic constant in the CWPO of TEB in different water matrix ($[\text{TEB}]_0 = 500 \text{ mg L}^{-1}$; $[\text{H}_2\text{O}_2]_0 = 2.7 \text{ mg L}^{-1}$; $\text{pH}_0 = 5$; $T = 25 \text{ }^\circ\text{C}$)

in degradation efficiency of azole pesticides may be associated with the presence of organic and inorganic

compounds in the treated water since they exhibit HO-scavenging properties (Bouanimba et al. 2015; Siedlecka et al. 2007). For example, the presence of salts such as bicarbonate or sulfate are well known to consume hydroxyl radicals, making them unavailable for pesticide oxidation. Even though sulfate and chloride radicals could be generated in these scavenging reactions, these radicals show a significantly lower oxidizing power than hydroxyl radicals (Dimitroula et al. 2012; Luo et al. 2014; Pignatello et al. 2006). On the other hand, the presence of organic species in the water matrix may cause competition with the pesticides for the active sites of the catalyst (Autin et al. 2013; Fan et al. 2013; Ye et al. 2019). To enhance the performance of the system and increase the pesticide conversion to at least 80% in the real WWTP effluent, the space-time was increased up to $32 \text{ g}_{\text{cat}} \text{ min mL}^{-1}$. Under these conditions, similar pseudo-first apparent kinetic constant values were obtained compared with the achieved with deionized water at a lower space-time ($16 \text{ g}_{\text{cat}} \text{ min mL}^{-1}$). Consequently, by varying the space-time, comparable levels of conversion were obtained for the micropollutants when using deionized water. For instance, TEB exhibited a conversion of approximately 93% in deionized water, while a conversion of 91% was achieved using WWTP effluent. Furthermore, it must be noted that the system showed an outstanding stability, maintaining nearly consistent pesticide conversions throughout the 25-h experiment. In addition, the use of a real water matrix did not lead to carbonaceous deposits on the catalyst surface. Similarly, it was also verified that the use of a secondary effluent water matrix did not increase the concentration of dissolved iron compared to the use of ultrapure water ($< 0.05 \text{ wt}\%$).

Conclusions

The FBR packed with natural magnetite has demonstrated to be highly effective and remarkably stable for the removal of a representative mixture of azole pesticides in continuous long-term operation. A comprehensive study was carried out to demonstrate the absence of mass transfer rate limitations and thus, to confirm that the system takes place under chemical kinetic control. The performance of the process was successfully described by a pseudo-first-order kinetic equation. The stability of the system was confirmed under long-term continuous operating, not appreciating any catalytic deactivation upon 200 h on stream. On the other hand, a complete operating condition study was carried out. It should be noted that variations in both space–time and H_2O_2 concentration led to changes in pesticide conversions, but in any case, the stability of the system was affected. For instance, the increase of τ led to a significant increase on the oxidation conversion of the pollutants up to > 95%, consistent with the higher residence time. Also, decreasing the stoichiometric H_2O_2 dose by half led to a decrease on the oxidation rate of the azole pesticides, while its increase by half led to a slight increase. On the opposite, a further increase of the H_2O_2 up to 200% of the stoichiometric amount caused a poorer performance, which can be explained by a competitive effect for the catalytic active centers and oxidizing radicals. All in all, azole pesticide conversion values above 80% were achieved under selected operating conditions ($W_{Fe_3O_4} = 8$ g, $[H_2O_2]_0 = 6.7$ mg L⁻¹, flow rate = 0.5 mL min⁻¹, $pH_0 = 5$, $T = 25$ °C). Finally, the versatility of the process was demonstrated using a real WWTP effluent spiked with the mixture of pesticides. The reaction matrix did not have any negative effect on the stability of the system although it led to a lower oxidation rate, which could be overcome by increasing the space–time. Considering the outstanding stability exhibited by the proposed catalytic system in this work, future research in this field should be focused on its scale-up to a pilot plant to yield valuable insights and substantiate the potential application of the catalytic system on a larger scale.

Supplementary Information The online version contains supplementary material available at <https://doi.org/10.1007/s11356-024-33065-8>.

Author contribution Neus Lopez-Arago: writing—original draft, writing—review and editing, investigation, methodology, visualization. Macarena Munoz: conceptualization, writing—original draft, writing—review and editing, methodology, supervision, funding acquisition. Zahara M. de Pedro: conceptualization, writing—review and editing, methodology, supervision, project administration, funding acquisition. Jose A. Casas: conceptualization, writing—review and editing, methodology, supervision, project administration, funding acquisition.

Funding Open Access funding provided thanks to the CRUE-CSIC agreement with Springer Nature. This research has been supported by the Spanish Ministry of Science and Innovation and AEI

through the grant PID2019-105079RB-I00 funded by MCIN/AEI/10.13039/501100011033 and by ERDF A way of making Europe, and from the Community of Madrid through the project P2018/EMT-4341. M. Munoz thanks the Spanish AEI for the Ramón y Cajal postdoctoral contract (RYC-2016–20648) and N. Lopez-Arago for the FPI predoctoral grant (PRE2020-09452), funded by MCIN/AEI/10.13039/501100011033 and by ESF Investing in your future.

Data availability Data will be made available on request.

Declarations Ethical approval.

Not applicable.

Consent to participate Not applicable.

Consent for publication Not applicable.

Competing interests The authors declare no competing interests.

Open Access This article is licensed under a Creative Commons Attribution 4.0 International License, which permits use, sharing, adaptation, distribution and reproduction in any medium or format, as long as you give appropriate credit to the original author(s) and the source, provide a link to the Creative Commons licence, and indicate if changes were made. The images or other third party material in this article are included in the article's Creative Commons licence, unless indicated otherwise in a credit line to the material. If material is not included in the article's Creative Commons licence and your intended use is not permitted by statutory regulation or exceeds the permitted use, you will need to obtain permission directly from the copyright holder. To view a copy of this licence, visit <http://creativecommons.org/licenses/by/4.0/>.

References

- Ahmed MB, Zhou JL, Ngo HH, Guo W, Thomaidis NS, Xu J (2017) Progress in the biological and chemical treatment technologies for emerging contaminant removal from wastewater: a critical review. *J Hazard Mater* 323:274–298. <https://doi.org/10.1016/j.jhazmat.2016.04.045>
- Alalm MG, Djellabi R, Meroni D, Pirola C, Bianchi CL, Boffito DC (2021) Toward scaling-up photocatalytic process for multiphase environmental applications. *Catalysts* 11:562. <https://doi.org/10.3390/catal11050562>
- Autin O, Hart J, Jarvis P, MacAdam J, Parsons SA, Jefferson B (2013) The impact of background organic matter and alkalinity on the degradation of the pesticide metaldehyde by two advanced oxidation processes: UV/ H_2O_2 and UV/ TiO_2 . *Water Res* 47:2041–2049. <https://doi.org/10.1016/j.watres.2013.01.022>
- Ben W, Zhu B, Yuan X, Zhang Y, Yang M, Qiang Z (2018) Occurrence, removal and risk of organic micropollutants in wastewater treatment plants across China: comparison of wastewater treatment processes. *Water Res* 130:38–46. <https://doi.org/10.1016/j.watres.2017.11.057>
- Berberidou C, Kokkinos P, Poullos I, Mantzavinos D (2022) Homogeneous photo-Fenton degradation and mineralization of model and simulated pesticide wastewaters in lab- and pilot-scale reactors. *Catalysts* 12:1512. <https://doi.org/10.3390/catal12121512>
- Bouanimba N, Laid N, Zouaghi R, Sehili T (2015) Effect of pH and inorganic salts on the photocatalytic decolorization of methyl orange in the presence of TiO_2 P25 and PC500. *Desalination Water Treat* 53:951–963. <https://doi.org/10.1080/19443994.2013.848667>

- Cai QQ, Wu MY, Li R, Deng SH, Lee BCY, Ong SL, Hu JY (2020) Potential of combined advanced oxidation – biological process for cost-effective organic matters removal in reverse osmosis concentrate produced from industrial wastewater reclamation: screening of AOP pre-treatment technologies. *Chem Eng J* 389:123419. <https://doi.org/10.1016/j.cej.2019.123419>
- Chen ZF, Ying GG (2015) Occurrence, fate and ecological risk of five typical azole fungicides as therapeutic and personal care products in the environment: a review. *Environ Int* 84:142–153. <https://doi.org/10.1016/j.envint.2015.07.022>
- di Luca C, Massa P, Grau JM, Marchetti SG, Fenoglio R, Haure P (2018) Highly dispersed Fe^{3+} - Al_2O_3 for the Fenton-like oxidation of phenol in a continuous up-flow fixed bed reactor. Enhancing catalyst stability through operating conditions. *Appl Catal B* 237:1110–1123. <https://doi.org/10.1016/j.apcatb.2018.05.032>
- Dimitroula H, Daskalaki VM, Frontistis Z, Kondarides DI, Panagiotopoulou P, Xekoukoulotakis NP, Mantzavinos D (2012) Solar photocatalysis for the abatement of emerging micro-contaminants in wastewater: synthesis, characterization and testing of various TiO_2 samples. *Appl Catal B* 117–118:283–291. <https://doi.org/10.1016/j.apcatb.2012.01.024>
- Ding D, Tian P, Cao C, Sun Y, Xu J, Han YF (2020) Degradation of MO and H_2O_2 on $\text{Cu}/\gamma\text{-Al}_2\text{O}_3$ pellets in a fixed bed reactor: kinetics and transport characteristics. *AIChE J* 66:e17000. <https://doi.org/10.1002/aic.17000>
- Esteves BM, Morales-Torres S, Maldonado-Hódar FJ, Madeira LM (2022) Sustainable iron-olive stone-based catalysts for Fenton-like olive mill wastewater treatment: development and performance assessment in continuous fixed-bed reactor operation. *Chem Eng J* 435:134809. <https://doi.org/10.1016/j.cej.2022.134809>
- Esteves BM, Rodrigues CSD, Boaventura RAR, Maldonado-Hódar FJ, Madeira LM (2016) Coupling of acrylic dyeing wastewater treatment by heterogeneous Fenton oxidation in a continuous stirred tank reactor with biological degradation in a sequential batch reactor. *J Environ Manage* 166:193–203. <https://doi.org/10.1016/j.jenvman.2015.10.008>
- Fan C, Horng CY, Li SJ (2013) Structural characterization of natural organic matter and its impact on methomyl removal efficiency in Fenton process. *Chemosphere* 93:178–183. <https://doi.org/10.1016/j.chemosphere.2013.05.027>
- Farzaneh Kondori F, Badii K, Masoumi ME, Golkarnarenji G (2018) A novel continuous magnetic nano- Fe_3O_4 /perlite fixed bed reactor for catalytic wet peroxide oxidation of dyes: reactor structure. *Int J Environ Sci Technol* 15:543–550. <https://doi.org/10.1007/s13762-017-1420-1>
- Figuière R, Waara S, Ahrens L, Golovko O (2022) Risk-based screening for prioritisation of organic micropollutants in Swedish freshwater. *J Hazard Mater* 429:128302. <https://doi.org/10.1016/j.jhazmat.2022.128302>
- García L, Leyva-Díaz JC, Díaz E, Ordóñez S (2021) A review of the adsorption-biological hybrid processes for the abatement of emerging pollutants: removal efficiencies, physicochemical analysis, and economic evaluation. *Sci Total Environ* 780:146554. <https://doi.org/10.1016/j.scitotenv.2021.146554>
- García-Costa AL, Silveira JE, Zazo JA, Dionysiou DD, Casas JA (2021) Graphite as catalyst for UV-A LED assisted catalytic wet peroxide oxidation of ibuprofen and diclofenac. *Chem Eng J Adv* 6:100090. <https://doi.org/10.1016/j.cej.2021.100090>
- Hoffman, J.I. (1945) Review: colorimetric determination of traces of metals reviewed work(s): colorimetric determination of traces of metals, new series. JSTOR, <http://www.jstor.org/stable/1672652> (accessed 15 September 2022).
- Huacalco-Aguilar Y, Álvarez-Torrellas S, Larriba M, Águeda VI, Delgado JA, Ovejero G, Peres JA, García J (2021a) Naproxen removal by CWPO with Fe_3O_4 /multi-walled carbon nanotubes in a fixed-bed reactor. *J Environ Chem Eng* 9:105110. <https://doi.org/10.1016/j.jece.2021.105110>
- Huacalco-Aguilar Y, Diaz de Tuesta JL, Álvarez-Torrellas S, Gomes HT, Larriba M, Ovejero G, García J (2021b) New insights on the removal of diclofenac and ibuprofen by CWPO using a magnetite-based catalyst in an up-flow fixed-bed reactor. *J Environ Manage* 281:111913. <https://doi.org/10.1016/j.jenvman.2020.111913>
- Jørgensen LN, Heick TM (2021) Azole use in agriculture, horticulture, and wood preservation – is it indispensable? *Front Cell Infect Microbiol* 11:730297. <https://doi.org/10.3389/fcimb.2021.730297>
- Lewis KA, Tzilivakis J, Warner DJ, Green A (2016) An international database for pesticide risk assessments and management. *Hum Ecol Risk Assess* 22:1050–1064. <https://doi.org/10.1080/10807039.2015.1133242>
- Lipczynska-Kochany E, Sprah G, Harms S (1995) Influence of some groundwater and surface waters constituents on the degradation of 4-chlorophenol by the Fenton reaction. *Chemosphere* 30:9–20. [https://doi.org/10.1016/0045-6535\(94\)00371-Z](https://doi.org/10.1016/0045-6535(94)00371-Z)
- Liu F, Zhang H, Yan Y, Huang H (2020) Graphene as efficient and robust catalysts for catalytic wet peroxide oxidation of phenol in a continuous fixed-bed reactor. *Sci Total Environ* 701:134772. <https://doi.org/10.1016/j.scitotenv.2019.134772>
- Lopez-Arago N, Nieto-Sandoval J, Munoz M, de Pedro ZM, Casas JA (2023) Insights on the removal of the azole pesticides included in the EU Watch List by catalytic wet peroxide oxidation. *Environ Technol Innov* 29:103004. <https://doi.org/10.1016/j.eti.2022.103004>
- Lu MC, Chang YF, Chen IM, Huang YY (2005) Effect of chloride ions on the oxidation of aniline by Fenton's reagent. *J Environ Manage* 75:177–182. <https://doi.org/10.1016/j.jenvman.2004.12.003>
- Luo Y, Guo W, Ngo HH, Nghiem LD, Hai FI, Zhang J, Liang S, Wang XC (2014) A review on the occurrence of micropollutants in the aquatic environment and their fate and removal during wastewater treatment. *Sci Total Environ* 473–474:619–641. <https://doi.org/10.1016/j.scitotenv.2013.12.065>
- Mailler R, Gasperi J, Coquet Y, Derome C, Buleté A, Vulliet E, Bressy A, Varrault G, Chebbo G, Rocher V (2016) Removal of emerging micropollutants from wastewater by activated carbon adsorption: experimental study of different activated carbons and factors influencing the adsorption of micropollutants in wastewater. *J Environ Chem Eng* 4:1102–1109. <https://doi.org/10.1016/j.jece.2016.01.018>
- Miklos DB, Remy C, Jekel M, Linden KG, Drewes JE, Hübner U (2018) Evaluation of advanced oxidation processes for water and wastewater treatment – a critical review. *Water Res* 139:118–131. <https://doi.org/10.1016/j.watres.2018.03.042>
- Miyawaki T, Nishino T, Asakawa D, Haga Y, Hasegawa H, Kadokami K (2021) Development of a rapid and comprehensive method for identifying organic micropollutants with high ecological risk to the aquatic environment. *Chemosphere* 263:128258. <https://doi.org/10.1016/j.chemosphere.2020.128258>
- Munoz M, Conde J, de Pedro ZM, Casas JA (2018) Antibiotics abatement in synthetic and real aqueous matrices by H_2O_2 /natural magnetite. *Catal Today* 313:142–147. <https://doi.org/10.1016/j.cattod.2017.10.032>
- Munoz M, de Pedro ZM, Casas JA, Rodriguez JJ (2015) Preparation of magnetite-based catalysts and their application in heterogeneous Fenton oxidation - a review. *Appl Catal B* 176:249–265. <https://doi.org/10.1016/j.apcatb.2015.04.003>
- Munoz M, De Pedro ZM, Casas JA, Rodriguez JJ (2014) Combining efficiently catalytic hydrodechlorination and wet peroxide oxidation (HDC-CWPO) for the abatement of organochlorinated water pollutants. *Appl Catal B* 150–151:197–203. <https://doi.org/10.1016/j.apcatb.2013.12.029>

- Pera-Titus M, García-Molina V, Baños MA, Giménez J, Esplugas S (2004) Degradation of chlorophenols by means of advanced oxidation processes: a general review. *Appl Catal B* 47:219–256. <https://doi.org/10.1016/j.apcatb.2003.09.010>
- Pesce S, Zoghlami O, Margoum C, Artigas J, Chaumot A, Foulquier A (2016) Combined effects of drought and the fungicide tebuconazole on aquatic leaf litter decomposition. *Aquat Toxicol* 173:120–131. <https://doi.org/10.1016/j.aquatox.2016.01.012>
- Pignatello JJ, Oliveros E, MacKay A (2006) Advanced oxidation processes for organic contaminant destruction based on the fenton reaction and related chemistry. *Crit Rev Environ Sci Technol* 36:1–84. <https://doi.org/10.1080/10643380500326564>
- Pinchao G, Ortiz L, Galeano LA, Hidalgo A, Ramírez JH (2021) Optimized CWPO oxidation of natural organic matter in continuous fixed bed reactor catalyzed by an extruded Al/Fe-PILC clay catalyst. *J Environ Chem Eng* 9:104634. <https://doi.org/10.1016/j.jece.2020.104634>
- Pliego G, Zazo JA, Blasco S, Casas JA, Rodriguez JJ (2012) Treatment of highly polluted hazardous industrial wastewaters by combined coagulation - adsorption and high-temperature fenton oxidation. *Ind Eng Chem Res* 51:2888–2896. <https://doi.org/10.1021/ie202587b>
- Poulsen R, Luong X, Hansen M, Styrisshave B, Hayes T (2015) Tebuconazole disrupts steroidogenesis in *Xenopus laevis*. *Aquat Toxicol* 168:28–37. <https://doi.org/10.1016/j.aquatox.2015.09.008>
- Rokbani O, Fattouch S, Chakir A, Roth E (2019) Heterogeneous oxidation of two triazole pesticides (dimiconazole and tebuconazole) by OH-radicals and ozone. *Sci Total Environ* 694:133745. <https://doi.org/10.1016/j.scitotenv.2019.133745>
- Saravanan A, Senthil Kumar P, Jeevanantham S, Karishma S, Tajsabreen B, Yaashikaa PR, Reshma B (2021) Effective water/wastewater treatment methodologies for toxic pollutants removal: processes and applications towards sustainable development. *Chemosphere* 280:130595. <https://doi.org/10.1016/j.chemosphere.2021.130595>
- Serrano E, Munoz M, de Pedro ZM, Casas JA (2020) Fast oxidation of the neonicotinoid pesticides listed in the EU Decision 2018/840 from aqueous solutions. *Sep Purif Technol* 235:116168. <https://doi.org/10.1016/j.seppur.2019.116168>
- Serrano E, Munoz M, de Pedro ZM, Casas JA (2019) Efficient removal of the pharmaceutical pollutants included in the EU Watch List (Decision 2015/495) by modified magnetite/H₂O₂. *Chem Eng J* 376:120265. <https://doi.org/10.1016/j.cej.2018.10.202>
- Siedlecka EM, Wieckowska A, Stepnowski P (2007) Influence of inorganic ions on MTBE degradation by Fenton's reagent. *J Hazard Mater* 147:497–502. <https://doi.org/10.1016/j.jhazmat.2007.01.044>
- Stamatis N, Antonopoulou M, Konstantinou I (2015) Photocatalytic degradation kinetics and mechanisms of fungicide tebuconazole in aqueous TiO₂ suspensions. *Catal Today* 252:93–99. <https://doi.org/10.1016/j.cattod.2014.09.023>
- Stamatis N, Hela D, Konstantinou I (2010) Occurrence and removal of fungicides in municipal sewage treatment plant. *J Hazard Mater* 175:829–835. <https://doi.org/10.1016/j.jhazmat.2009.10.084>
- Storck V, Nikolaki S, Perruchon C, Chabanis C, Sacchi A, Pertile G, Baguelin C, Karas PA, Spor A, Devers-Lamrani M, Papadopoulou ES, Sibourg O, Malandain C, Trevisan M, Ferrari F, Karpouzias DG, Tsiamis G, Martin-Laurent F (2018) Lab to field assessment of the ecotoxicological impact of chlorpyrifos, isoproturon, or tebuconazole on the diversity and composition of the soil bacterial community. *Front Microbiol* 9:1412. <https://doi.org/10.3389/fmicb.2018.01412>
- Thirumoorthy K, Gokulakrishnan B, Satishkumar G, Landau MV, Man MWC, Oliviero E (2021) Al-Doped magnetite encapsulated in mesoporous carbon: a long-lasting Fenton catalyst for CWPO of phenol in a fixed-bed reactor under mild conditions. *Catal Sci Technol* 11:7368–7379. <https://doi.org/10.1039/d1cy01218e>
- Vega G, Quintanilla A, López P, Belmonte M, Casas JA (2022) Structured reactors based on 3D Fe/SiC catalysts: understanding the effects of mixing. *Ind Eng Chem Res* 61:11678–11690. <https://doi.org/10.1021/acs.iecr.2c01611>
- Yang Y, Zhang H, Yan Y (2018) Catalytic wet peroxide oxidation of m-cresol over novel Fe₂O₃ loaded microfibrillar entrapped CNT composite catalyst in a fixed-bed reactor. *J Chem Technol Biotechnol* 93:2552–2563. <https://doi.org/10.1002/jctb.5609>
- Ye Y, Bruning H, Liu W, Rijnaarts H, Yntema D (2019) Effect of dissolved natural organic matter on the photocatalytic micropollutant removal performance of TiO₂ nanotube array. *J Photochem Photobiol A Chem* 371:216–222. <https://doi.org/10.1016/j.jphotochem.2018.11.012>

Publisher's Note Springer Nature remains neutral with regard to jurisdictional claims in published maps and institutional affiliations.